Acta Crystallographica Section B
Structural Science
ISSN 0108-7681

Invariom structure refinement, electrostatic potential and toxicity of 4-*O*-methylalpinumisoflavone, *O*,*O*-dimethylalpinumisoflavone and 5-*O*-methyl-4-*O*-(3-methylbut-2-en-1-yl)alpinumisoflavone

Robert Kingsford-Adaboh,[a]* Birger Dittrich,[b] Christian B. Hübschle,[c] Winfred S. K. Gbewonyo,[d] Hideki Okamoto,[e] Masaro Kimura[e] and Hiroyuki Ishida[e]

[a]Department of Chemistry, University of Ghana, LG 56 Legon, Accra, Ghana, [b]Department of Chemistry, M313, University of Western Australia, Crawley, WA 6009, Australia, [c]Institut für Chemie/Kristallographie, Freie Universität Berlin, 14195 Berlin, Germany, [d]Department of Biochemistry, University of Ghana, LG 56 Legon, Accra, Ghana, and [e]Department of Chemistry, Faculty of Science, Okayama University, Okayama, Japan

Correspondence e-mail: kadabohs@ug.edu.gh

Received 11 January 2006
Accepted 25 May 2006

The accurate X-ray single-crystal structures of the isoflavone compounds 4-*O*-methylalpinumisoflavone, *O*,*O*-dimethylalpinumisoflavone and 5-*O*-methyl-4-*O*-(3-methylbut-2-en-1-yl)alpinumisoflavone {alpinumisoflavone = 5-hydroxy-7-(4-hydroxyphenyl)-2,2-dimethyl-2*H*,6*H*-benzo[1,2-*b*:5,4-*b*′]-dipyran-6-one} from data sets measured at cryogenic temperature have been obtained from invariom modelling using theoretically predicted Hansen and Coppens multipole-model form factors, which describe the aspherical electron density distribution. Molecular dipole moments and electrostatic potentials obtained from invariom modelling are discussed and compared with results from *ab initio* theoretical calculations. All three studied compounds are solvent extracts of root bark or seed powder of *Millettia thonningii* (*leguminosae*), a plant molluscicide and cercaricide used in Franco West Africa as medication against various diseases. The compounds' toxicities to brine shrimp have been determined and their different potencies tentatively related to conformation differences, intramolecular contacts, dipole moments and electrostatic potential features.

1. Introduction

In this study the X-ray single-crystal structures of three compounds obtained from dichloromethane extracts of the seeds of *Milletia thonningii* were investigated. This study forms part of the systematic characterization of the crystal structures of petrol extracts of *M. thonningii* Baker from its root bark or seeds (Kingsford-Adaboh *et al.*, 2001, 2006), with the hope that the crystal structure and molecular and electronic properties can further deepen our understanding of their observed bioactivities. In Franco West Africa the bark infusion is used as a laxative for children (Irvine, 1961). The pulverized roots and bark decoction is drunk in Nigeria as relief for menstrual pains, as a blood purifier and also as a de-wormer. The leaf extract is used in Nigeria as a cure for dysentery and diarrhoea (Irvine, 1961; Abbiw, 1990). More importantly, the leaf juice is reported to be lethal to Bulinus snail (Abbiw, 1990; Maillard *et al.*, 1993), a water snail carrying the microorganisms that cause schistosomiasis-bilharzias, a parasitic disease endemic throughout South America, Africa and the Far East (Maillard *et al.*, 1993). Lyddiard and Whitfield mention an inhibitory effect on the site I mitochondrial electron transport system (Lyddiard & Whitfield, 2001) and anti-schistosomal bioactivity (Lyddiard *et al.*, 2002) of extracts of *M. thonningii* on *Schistosoma mansoni* miracidia, cercariae and worms. Although a

dichloromethane solution of the isoflavones is reported to elicit the observed activities, it is unknown as to which of the many possible isoflavones are responsible and how the presence, absence or relative position of functional groups as well as differences in molecular conformation are linked to their activity.

Recent published studies have shown that the concept of invariom (Dittrich *et al.*, 2004, 2006) can be successfully used to model the aspherical electron densities of X-ray single-crystal structures, even when only low-order data are available. In this approach, the Hansen and Coppens multipole formalism (Hansen & Coppens, 1978) is used. For invariom modelling, theoretically predicted multipole populations of intermolecular transferable pseudoatoms (invariom) are stored in a database and provide an aspherical scattering model in contrast to the spherically symmetric independent atom model (IAM) density. This aspherical scattering model is used for an improved interpretation of conventional X-ray diffraction data. An invariom-based structure refinement leads to more precise atomic positions, especially for H atoms (Dittrich *et al.*, 2005), and to physically more meaningful anisotropic displacement parameters (x, y, z and U^{ij}). Furthermore, properties derived from the non-spherical electron density, like the electrostatic potential (ESP), can be calculated at low computational cost. The invariom method is based on the approximation of locality of molecular electron density. It is rationalized within the nearest-neighbour approximation (Koritsánszky *et al.*, 2002) that is extended to include one further shell of neighbours for H atoms or in delocalized systems. Thus, for each element in the periodic table only a limited number of invariom exist.

For the three title compounds, and more generally for the class of compounds of isoflavones, crystallization yields mostly soft and weakly diffracting crystals for which charge-density data sets cannot usually be measured in a normal X-ray laboratory. Using the invariom approach we are able to obtain a precise charge-density quality molecular geometry and a molecular electrostatic potential similar to the theoretically predicted one at low computational cost.

2. Experimental

2.1. Sample preparation and crystallization

Seeds of *M. thonningii* collected from the University of Ghana Botanical Gardens were air dried. These were ground into powder which was continuously soxhlet-extracted in methanol. Column chromatography and preparative thin-layer chromatography yielded compounds (2) and (3), *O*,*O*-dimethylalpinumisoflavone and 5-*O*-methyl-4-*O*-(3-methylbut-2-en-1-yl)alpinumisoflavone, respectively. Compound (1), 4-*O*-methylalpinumisoflavone, which hitherto had been difficult to crystallize for X-ray diffraction purposes, was obtained from demethylating a product of (2) in a mixture of cold BCl_3 and chloroform. IR and NMR spectra confirmed the methylated product. All three samples were crystallized from ethanol.

Table 1
Experimental table.

	(1)	(2)	(3)
Crystal data			
Chemical formula	$C_{21}H_{18}O_5$	$C_{22}H_{20}O_5$	$C_{52}H_{52}O_{10}$
M_r	350.35	364.38	836.94
Cell setting, space group	Monoclinic, $P2_1/c$	Monoclinic, $P2_1/n$	Orthorhombic, $Pna2_1$
Temperature (K)	90	90	120
a, b, c (Å)	8.3670 (2), 8.4724 (2), 23.6852 (5)	9.0604 (7), 19.0147 (14), 10.5963 (8)	11.9602 (3), 18.6249 (5), 19.9648 (5)
α, β, γ (°)	90, 92.5140 (10), 90	90, 101.333 (2), 90	90, 90, 90
V (Å^3)	1677.39 (7)	1789.9 (2)	4447.3 (2)
Z	4	4	4
D_x (Mg m^{-3})	1.387	1.356	1.250
Radiation type	Mo $K\alpha$	Mo $K\alpha$	Mo $K\alpha$
μ (mm^{-1})	0.10	0.10	0.09
Crystal form, colour	Plate-like, yellow	Plate-like, colourless	Prismatic, colourless
Crystal size (mm)	0.25 × 0.10 × 0.06	0.15 × 0.12 × 0.08	0.31 × 0.30 × 0.21
Data collection			
Diffractometer	CCD area detector	CCD area detector	CCD area detector
Data collection method	φ and ω scans	φ and ω scans	φ and ω scans
Absorption correction	Empirical (using intensity measurements)	Empirical (using intensity measurements)	Empirical (using intensity measurements)
T_{min}	0.976	0.978	0.974
T_{max}	0.994	0.990	0.982
No. of measured, independent and observed reflections	47 225, 7659, 5021	29 061, 8631, 5234	114 385, 10 408, 8668
Criterion for observed reflections	$F > 2\sigma(F)$	$I > 2\sigma(I)$	$F > 2\sigma(F)$
R_{int}	0.071	0.066	0.063
θ_{max} (°)	35.5	36.3	35.5
Refinement			
Refinement on $R[F^2 > 2\sigma(F^2)]$, $wR(F^2)$, S	F 0.030, 0.021, 1.14	F 0.043, 0.028, 1.30	F 0.029, 0.021, 1.59
No. of reflections	5021	5234	8668
No. of parameters	307	324	764
H-atom treatment	Refined independently	Refined independently	Refined independently
Weighting scheme	$w1 = 1/[\sigma^2(F_o)]$	$w1 = 1/[\sigma^2(F_o)]$	$w1 = 1/[\sigma^2(F_o)]$
$(\Delta/\sigma)_{max}$	<0.0001	<0.0001	<0.0001
$\Delta\rho_{max}$, $\Delta\rho_{min}$ (e Å^{-3})	0.32, −0.18	0.29, −0.27	0.33, −0.18

Computer programs: *SMART*, *SAINT*, *SADABS* (Bruker AXS Inc. 2002), *SHELXS*97 (Sheldrick, 1990), *XD* (Koritsánszky *et al.*, 2003).

2.2. X-ray diffraction experiments

Single-crystal X-ray diffraction experiments were carried out using Mo $K\alpha$ radiation on a Bruker APEX I CCD diffractometer equipped with a nitrogen-gas-stream cooling device at cryogenic temperature. Although the crystals were diffracting relatively weakly, a good resolution and coverage

was achieved. The crystal-to-detector distance was set to 4.5 cm. Reciprocal space was explored by a combination of various ω and φ scans and each frame covered 0.6°. The detector was positioned at different 2θ values according to measurement strategies planned with *COSMO* (Bruker AXS, 2002). The radiation time per frame was different for the three compounds. For (1) frames were radiated for 5 s, while for substance (2) the duration was 60 s. For (3) the radiation time per frame was 30 s. Details of crystal data and measurement conditions are given in Table 1.[1]

Compounds (1) and (2) crystallize in centrosymmetric space groups with one molecule per unit cell, whereas the space group for (3) is $Pna2_1$, with two independent molecules in the asymmetric unit. An overlay of these two molecules reveals very similar conformations, that differ mainly in the orientation of the $-CH_2CH{=}C(Me)_2$ group, which is rotated by $\sim$180° in molecule *B* with respect to molecule *A*.

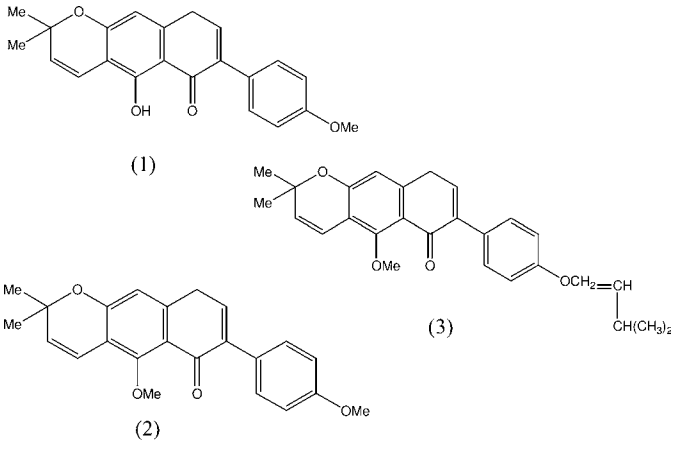

2.3. Toxicity of the isolated compounds to brine shrimp

Brine shrimp, *Artemia salina* Leach, has been successfully used as a bench-top assay to determine the toxicity levels of natural products from plants (Meyer *et al.*, 1982), as brine shrimp larvae are sensitive to small doses of biologically active chemicals. Eggs of brine shrimp (Brine Shrimp Direct, California, USA) were hatched in sea salt water (3.8%) and were allowed to hatch and mature for 48 h, before nauplii were used for a bioassay,[2] in which dilutions of the compounds ranging between 0.01 and 100 µg ml^{-1} were used.

[1] Supplementary data for this paper are available from the IUCr electronic archives (Reference: SN5034). Services for accessing these data are described at the back of the journal.

[2] 5 µl of each concentration were aliquoted separately into 10 ml vials, evaporated under a stream of nitrogen gas, and the residue was dissolved with 40 µl of acetone. Sea water (2 ml) was initially added, followed by transfer of ten brine shrimp nauplii to each vial, with the volume being finally made up to 5 ml with additional sea water. Control vials containing only 40 µl of acetone and ten brine shrimp in 5 ml of sea water were also set up. Each test was replicated four times and the number of dead shrimp nauplii after 24 h was recorded. The results were analyzed using *MINITAB* (version 12 for Windows) software. Abbots formula (Abbott, 1925) was used to correct for natural mortality.

3. Invariom refinement

For the representation of the aspherical electron density the Hansen and Coppens multipole model (Hansen & Coppens, 1978) was used. Starting atomic parameters for all three molecular structures were taken from the *SHELXL* spherical atom refinement (Sheldrick, 1997). Further least-squares refinement was carried out with the full-matrix least-squares program *XDLSM* of the *XD* program package (Koritsánszky *et al.*, 2003). As crystals were only weakly diffracting, despite the low temperature of the measurements, a charge-density study on the molecules using a conventional X-ray source was not feasible. The invariom approach was used (Dittrich *et al.*, 2004) to obtain a precise experimental molecular geometry and approximate properties derived from the aspherical electron density. During the modelling process each atom was assigned an invariom, as shown exemparily in Table 2 for (1); the assignments for the other two molecules are not shown because they are chemically similar. Also listed are the model compound for creating the database entry and the local atomic site symmetry assumed (Kurki-Suonio, 1977).

Invariom-multipole populations were not refined and the total molecular density was obtained by the summation of their contributions. The procedure for the build up of a database of theoretically derived multipole populations, as well as their notation, has been described recently (Dittrich *et al.*, 2005). Some improvements are mentioned: the geometry optimization of invariom model compounds with the program *GAUSSIAN*98 (Frisch *et al.*, 1998) uses the Dunning basis set D95++(3df,3pd). Employment of this basis set results in an improvement in the *R* factor for the data discussed here as well as the multi-temperature data of DL-serine when compared with all of the basis sets reported in that study (Dittrich *et al.*, 2005); for example, the Pople basis set 6-311++(3df,3pd).

Theoretical structure factors from the *GAUSSIAN* wavefunction by analytical Fourier transform of the Gaussian orbital products (Chandler & Spackman, 1978) using the program *TONTO* (Jayatilaka & Grimwood, 2003) are now generated for a 30 Å cubic cell to avoid density overlap.

When invariom modelling was originally introduced, H atoms were modelled by taking into account nearest neighbours only. It has been found that a better prediction of properties strongly influenced by the database monopole populations can be obtained when next-nearest neighbours are taken into account for H atoms. This reduces the deviation of the sum of the database monopole populations from electroneutrality (Dittrich *et al.*, 2006).

It has been emphasized that invariom can be automatically identified and assigned to the atom of interest from the atoms' connectivity, *i.e.* their nearest neighbours or, in the case of delocalized systems and H atoms, next-nearest neighbours. For this purpose, and for the transfer of the multipole populations and the coordinate system from the database, the preprocessor program *INVARIOMTOOL* has been used (Hübschle & Dittrich, 2004). In the least-squares refinement these database multipole parameters were not refined; the

Table 2
Invariom assigned to the atoms in (1) together with model compounds and the respective invariom-database symmetry.

Atom	Invariom assigned	Model compound	Database symmetry
O1	O1c1h	Methanol	*m*
O2	O2c	Formaldehyde	*m*
O3	O1c1c	Ether	*mm*2
O4	O1c1c	Ether	*mm*2
O5	O1c1c	Ether	*mm*2
C1	C1c1h1h1h	Ethane	3
C2	C1c1h1h1h	Ethane	3
C3	C1o1c1c1c	Isobutanol	3*m*
C4	C2c1c1h	Propene	*m*
C5	C2c1c1h	Propene	*m*
C6	C1.5c[1.5c1o]1.5c[1.5c1o]1c	1-Methyl-2,5-dihydroxybenzene	*mm*2
C7	C1.5c[1.5c1c]1.5c[1.5c1c]1o	1-Hydroxy,2,5-dimethylbenzene	*mm*2
C8	C1.5c[1.5c1o]1.5c[1.5c1o]1c	1-Methyl-2,5-dihydroxybenzene	*mm*2
C9	C2o1c1c	Acetone	*m*
C10	C2c1c1c	Isobutene	*m*
C11	C2c1o1h	Propenol	*m*
C12	C1.5c[1.5c1c]1.5c[1.5c1h]1o	1-Hydroxy-2-methylbenzene	*m*
C13	C1.5c[1.5c1o]1.5c[1.5c1o]1h	1,4-Dihydroxy-benzene	*mm*2
C14	C1.5c[1.5c1c]1.5c[1.5c1h]1o	1-Hydroxy-2-methylbenzene	*m*
C15	C1.5c[1.5c1h]1.5c[1.5c1h]1c	Toluene	*mm*2
C16	C1.5c[1.5c1c]1.5c[1.5c1h]1h	Toluene	*mm*2
C17	C1.5c[1.5c1o]1.5c[1.5c1h]1h	Phenol	*mm*2
C18	C1.5c[1.5c1h]1.5c[1.5c1h]1o	Phenol	*mm*2
C19	C1.5c[1.5c1o]1.5c[1.5c1h]1h	Phenol	*mm*2
C20	C1.5c[1.5c1c]1.5c[1.5c1h]1h	Toluene	*mm*2
C21	C1o1h1h1h	Methanol	3
H1	H1c[1c1h1h]	Ethane	6
H2	H1c[1c1h1h]	Ethane	6
H3	H1c[1c1h1h]	Ethane	6
H4	H1c[1c1h1h]	Ethane	6
H5	H1c[1c1h1h]	Ethane	6
H6	H1c[1c1h1h]	Ethane	6
H7	H1c[2c1c]	Propene	6
H8	H1c[2c1c]	Propene	6
H9	H1o[1c]	Methanol	6
H10	H1c[2c1o]	Propenol	6
H11	H1c[1.5c1.5c]	Benzene	6
H12	H1c[1.5c1.5c]	Benzene	6
H13	H1c[1.5c1.5c]	Benzene	6
H14	H1c[1.5c1.5c]	Benzene	6
H15	H1c[1.5c1.5c]	Benzene	6
H16	H1c[1o1h1h]	Methanol	6
H17	H1c[1o1h1h]	Methanol	6
H18	H1c[1o1h1h]	Methanol	6

number of refined parameters is therefore unchanged when compared with the IAM.

4. Results and discussion

4.1. Toxicity

All three compounds demonstrated lethal toxicity to brine shrimp nauplii as quantified with LD_{50}, which refers to the amount (*i.e.* lethal dose or concentration) of a substance that kills half of the test organisms. Compound (3), the 5-*O*-methyl derivative, was about 340 times as potent as the *O*,*O*-dimethyl derivative, which in turn was about 4.5 times as active as the 4-*O*-methyl derivative (see Table 3). The fact that the 5-*O*-methyl derivative gave over 1.5×10^3 times as much potency as (1), the 4-*O*-methyl derivative, is noteworthy. We found this potency to be slightly higher than rotenoids isolated from the seeds of *Millettia dura* Dunn (*Leguminosae*) against second-instar larvae of the mosquito, *Aedes aegypti* L (Diptera: Culicidae), with LD_{50} values between 1.4 and 1.6 $\mu g\ ml^{-1}$ at 24 h (Yenesew *et al.*, 2003).

Table 3
LD_{50} values of brine shrimp nauplii from a bioassay for (1), (2) and (3).

Compound	LD_{50} value
(1)	35.2 ± 6.0
(2)	7.7 ± 1.9
(3)	0.02 ± 0.01

Table 4
Refinement details and figures of merit for (1), (2) and (3).

	(1)	(2)	(3)
Refinement method	Full-matrix least squares on F		
Criterion for observed reflections	$2\sigma F$	$2\sigma F$	$2\sigma F$
Data included/parameters	5021/307	5243/324	8668/767
Weighting scheme	Based on measured s.u.'s†		
Figures of merit for IAM			
Goodness-of-fit S	1.97	1.88	2.56
$R(F)$ (%)	4.7	5.8	4.5
$R_w(F)$ (%)	3.6	4.0	3.4
Largest difference peak (e Å^{-3})	0.48	0.44	0.32
Largest difference hole (e Å^{-3})	−0.32	−0.38	−0.29
Figures of merit for invariom model			
Goodness-of-fit	1.14	1.30	1.59
$R(F)$ (%)	3.0	4.3	2.9
$R_w(F)$ (%)	2.1	2.8	2.1
Largest difference peak (e Å^{-3})	0.32	0.29	0.33
Largest difference hole (e Å^{-3})	−0.18	−0.27	−0.18

† $S = [\sum(||F_o| - k|F_c||)^2/(n_o - m_{var})]^{1/2}$, $R(F) = \sum ||F_o| - |F_c||/\sum |F_o|$, $R_w(F) = [\sum w||F_o| - k|F_c||^2/\sum w|F_o|^2]^{1/2}$, $w = 1/\sigma^2$.

4.2. Structure and dipole moment

Invariom refinement leads to a better fit of calculated to experimental structure factors. In Table 4 several figures of merit are compared for the independent atom and invariom models. The reduction of the R factor is remarkable for the latter. This is on the one hand due to the relatively high resolution of the data and on the other to the fact that the relative hydrogen content of the three molecules is high. Hydrogen scattering contributes, to a considerable extent, to differences between the IAM and invariom structure factors at low scattering angles. Furthermore, standard deviations in bond length (see Table 5) and angle are improved significantly and the residual density is reduced.

Figs. 1(*a*)–1(*c*) show *ORTEP* representations (Burnett & Johnson, 1996) of the three molecules.

For invariom refinements the anisotropic displacement parameters (ADPs) for the non-H atoms carry more physical information in contrast to the IAM, where the physical

Table 5
Hirshfeld test and bond-length shortening for (1) and average DMSDA for (2) and (3) for the invariom and independent atom models.

DMSDA is the difference of mean-square displacement amplitudes in units of 10×10^{-4} Å^2.

	Invariomes		Independent atom model	
Bond	Bond length	DMSDA	Bond length	DMSDA
O1—C7	1.3431 (8)	2	1.3515 (13)	−1
O2—C9	1.2579 (7)	11	1.2611 (13)	16
O3—C11	1.3400 (8)	−14	1.3481 (13)	4
O3—C12	1.3575 (7)	−11	1.3690 (13)	−8
O4—C3	1.4637 (8)	−6	1.4731 (13)	−11
O4—C14	1.3424 (8)	−6	1.3530 (13)	−9
O5—C18	1.3619 (8)	−9	1.3751 (13)	3
O5—C21	1.4283 (9)	3	1.4354 (14)	1
C1—C3	1.5235 (10)	0	1.5184 (17)	0
C2—C3	1.5238 (10)	4	1.5204 (17)	0
C3—C4	1.5010 (10)	−7	1.4993 (17)	9
C4—C5	1.3359 (10)	11	1.3256 (17)	6
C5—C6	1.4591 (9)	6	1.4573 (16)	−17
C6—C7	1.3935 (9)	4	1.3916 (15)	15
C6—C14	1.4128 (9)	8	1.4062 (15)	21
C7—C8	1.4224 (9)	1	1.4214 (15)	−18
C8—C9	1.4423 (9)	1	1.4422 (15)	22
C8—C12	1.4037 (9)	0	1.3993 (15)	13
C9—C10	1.4613 (9)	3	1.4646 (15)	−16
C10—C11	1.3589 (9)	−1	1.3523 (16)	20
C10—C15	1.4902 (9)	8	1.4849 (15)	−13
C12—C13	1.3875 (9)	−10	1.3782 (15)	−1
C13—C14	1.3901 (9)	6	1.3866 (15)	16
C15—C16	1.4041 (9)	6	1.4016 (15)	27
C15—C20	1.3983 (9)	3	1.3950 (15)	9
C16—C17	1.3872 (9)	1	1.3808 (16)	−16
C17—C18	1.4019 (9)	−1	1.3971 (15)	9
C18—C19	1.3955 (9)	−1	1.878 (15)	−8
C19—C20	1.3952 (9)	8	1.3907 (16)	3
DMSDA average		5.24		10.76
DMSDA average of (2)		8.70		10.53
Maximum DMSDA of (2)		22		30
DMSDA average of (3)		9.52		13.93
Maximum DMSDA of (3)		54†		59†

† Occurs at C1*A*—C3*A* and C2*A*—C3*A*; these methyl groups are possibly disordered.

meaning is subject to debate (Brock & Dunitz, 1982). The Hirshfeld test (Hirshfeld, 1976) allows the quality of the ADPs to be assessed. While in the IAM refinement 14, 15 and 40 bonds fail the 10×10^{-4} Å^2 limit for (1), (2) and (3), respectively, as suggested by Hirshfeld, only 5, 10 and 22 bonds fail for the respective invariom refinement.

Table 5 illustrates the improvement in the physical meaning of anisotropic displacement parameters exemplarily for (1). As mentioned before (Dittrich *et al.*, 2005), asphericity shifts (Coppens *et al.*, 1969) are corrected for, which for these molecules appear in the shorter invariom-model C—O and C═O bond lengths, but longer C═C bond lengths when compared with the IAM, where spherical averaging over the oxygen or carbon valence density biases results.

In this work our approach towards a better understanding of questions of structure–activity raised in the introduction is to calculate two properties from the aspherical density distribution as obtained with invariom modelling: the molecular dipole moment and the ESP. A similar comparison for a wider range of properties can be found in a recent paper by Volkov *et al.* (2004), who base their predictions on a similar

Table 6
Dipole moments for (1), (2) and (3).

Compound	Method	Total dipole moment (D)
(1)	Invariom database	3.5
	B3LYP/D95++(3df,3pd)	3.7
(2)	Invariom database	3.9
	B3LYP/D95++(3df,3pd)	3.2
(3) (molecule *A*)	Invariom database	5.4
	B3LYP/D95++(3df,3pd)	3.9
(3) (molecule *B*)	Invariom database	2.5
	B3LYP/D95++(3df,3pd)	2.7

database where multipole parameters were averaged. They reported that the accuracy of the moments calculated from the database is of the same order as the differences between various *ab initio* methods.

In Table 6 the magnitudes of the dipole moments of the three compounds are listed and compared with theoretical single-point calculations at the B3LYP level of theory with the basis set D95++(3df,3pd), available from the program *GAUSSIAN* (Frisch *et al.*, 1998) using the experimental invariom geometry. This basis set had also been used for the generation of database entries. Invariom database results are in satisfactory agreement with their theoretical counterparts. Differences in the dipole moment for the two conformers of (3) show that relatively small changes in conformation can influence the resulting dipole moment considerably. More studies on smaller, more polar, systems would be useful to

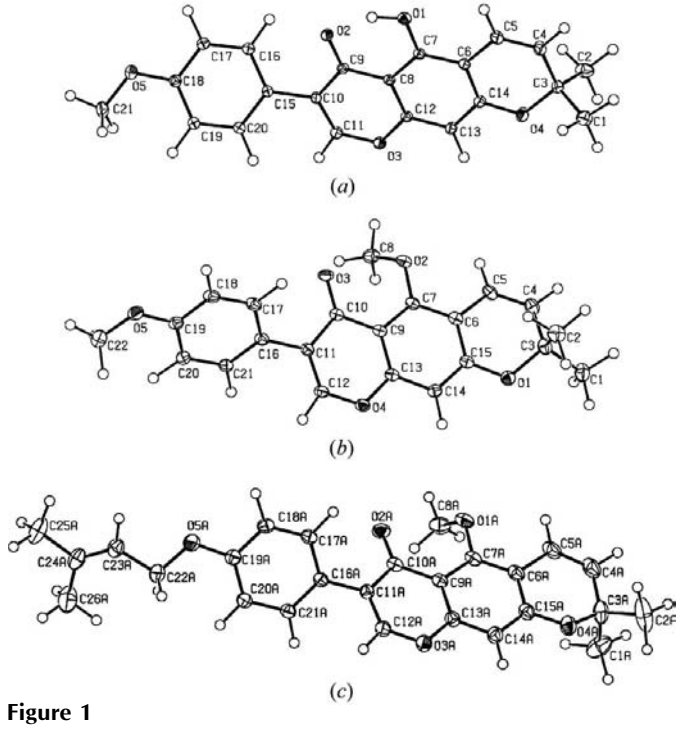

Figure 1
ORTEP representation (Burnett & Johnson, 1996) of the experimentally determined molecular structures in the crystal with atomic numbering schemes. Displacement ellipsoids are drawn at the 50% probability level. (*a*) Compound (1); (*b*) (2); (*c*) (3). For the latter, only one of the two similar molecules in the asymmetric unit is shown.

Table 7
Intermolecular/intramolecular contacts (for $D\cdots A \leq 3.3$ Å) for (1), (2) and (3).

Molecule	D—H$\cdots A$	Symmetry code	D—H	H$\cdots A$	$D\cdots A$
(1)	O1—H9$\cdots$O2	Intra	0.987 (6)	1.669 (8)	2.5822 (7)
	C16—H12$\cdots$O2	Intra	1.088 (8)	2.457 (8)	2.9678 (8)
(2)	C8—H11$\cdots$O3	Intra	1.00 (2)	2.30 (2)	2.951 (2)
	C17—H14$\cdots$O3	Intra	1.09 (1)	2.568 (15)	2.9927 (9)
	C20—H19$\cdots$O2	$-1/2+x, 3/2-y, -1/2+z$	1.12 (1)	2.589 (12)	3.1791 (11)
	C21—H20$\cdots$O2	$-1/2+x, 3/2-y, -1/2+z$	1.08 (1)	2.500 (13)	3.1841 (11)
(3)	C4A—H7$A\cdots$O1B	$1/2-x, -1/2+y, -1/2+z$	1.01 (2)	2.40 (2)	3.251 (2)
	C8A—H11$A\cdots$O2A	Intra	1.02 (2)	2.46 (2)	2.878 (2)
	C8B—H11$B\cdots$O2B	Intra	1.03 (2)	2.556 (14)	2.976 (2)
	C17A—H14$A\cdots$O2A	Intra	1.05 (1)	2.55 (2)	2.9376 (14)
	C17B—H14$B\cdots$O2B	Intra	1.11 (2)	2.55 (2)	2.9595 (14)
	C21A—H17$A\cdots$O2A	$1/2+x, 1/2-y, z$	1.03 (2)	2.410 (13)	3.2384 (12)

clarify how accurately the individual components of the dipole moment can be predicted from the invariom database.

Conformational and structural analysis of the 5-*O*-methyl derivative (3) shows it to have features intermediate between (1), the 4-*O*-methyl derivative, and (2), the *O*,*O*-dimethyl derivative (Kingsford-Adaboh *et al.*, 2006). The methoxy group substitution at C7 and the much bulkier substitution of the $-CH_2CH{=}C(Me)_2$ functional group at C19 could be responsible for the large disparity between the measured potencies of (3) and (1). By a similar argument, the nature and type of the functional group substitution may also explain the observed higher activity of the *O*,*O*-dimethyl derivative (2) over the 4-*O*-methyl derivative (1). The substitution by the unsaturated molecular fragment affords the 5-*O*-methyl derivative to show more intramolecular contacts amongst the three compounds as shown in Table 7, which could be a contributory factor in the observed phenomenon.

4.3. Electrostatic potential

Volkov *et al.* (2004) have compared a quantum mechanical ESP derived from an extended basis-set calculation with the result of the database approach and reported that both methods correctly represent the sign of the ESP in all regions of the example molecule glutamine. Figs. 2(*a*1) and 2(*a*2) show an analogous comparison of (1) based on the same single-point energy calculation with the basis set D95++(3df,3pd) mentioned above for the calculation of the dipole moment. A qualitative agreement is obtained and all features of the potential are well reproduced in the ESP from the multipole-projected electron density of the invariom database that was calculated using the method of Su & Coppens (1992). The fact that the ESP can be obtained within minutes from invariom modelling, whereas even a single-point energy theoretical calculation is computationally demanding for bigger molecules, makes this approach suitable for a comparison of a series of molecules in cases where their structural data are available.

Figs. 2(*a*2), 2(*b*) and 2(*c*) show the ESP of the three molecules from the database using the same scale. Rather than ESP iso-surface representations, all four parts of Fig. 2 show the ESP mapped onto an iso-surface of the electron density of 0.5 e Å^{-3} using the program *MOLISO*, which is currently under development (Hübschle, 2006).

Differences in the ESP of the three molecules are most pronounced at atom O5, which is affected by substitution at C19. Replacing the methyl functional group with a $-CH_2CH{=}C(Me)_2$ group has more effect than replacing the H atom at O1 in (1) with a methyl group. Still, the differences are relatively small and the observed higher activity of (2) and (3) with respect to (1) will probably, to a considerable extent, be influenced by molecular conformation, shape and dimensions. From a more general point of view the question as to how far the interaction between the ESP of a receptor and a substrate is enhanced when two conformationally similar

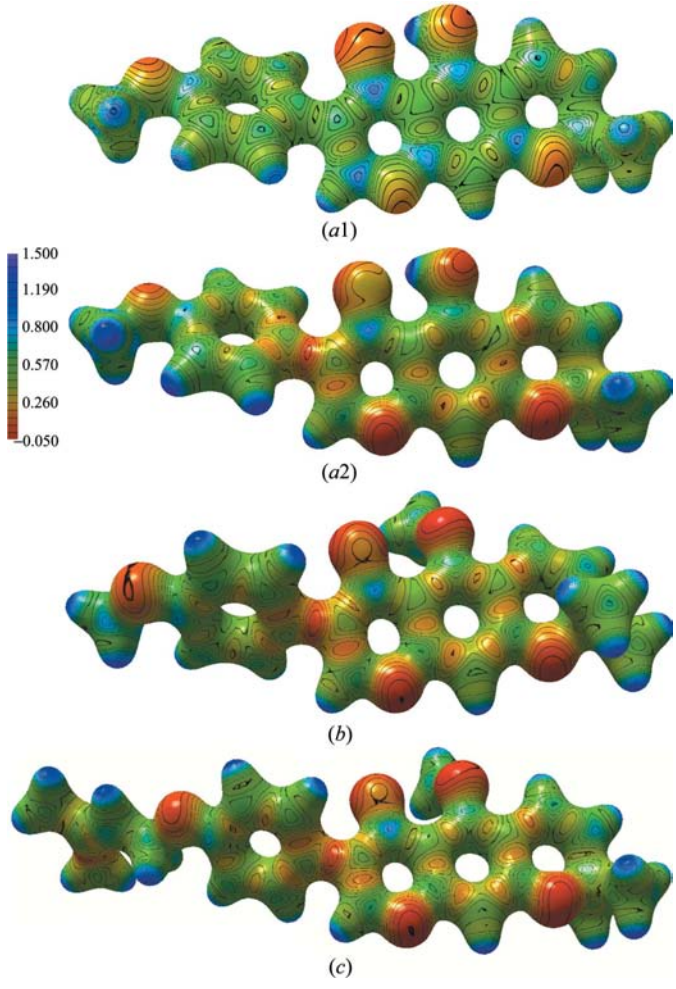

Figure 2
Electrostatic potential of the three molecules, all mapped on an 0.5 e Å^{-3} iso-surface of electron density using the same scale (maximum negative value: -0.05 e Å^{-1}; maximum positive value: 1.5 e Å^{-1} according to colour code). (*a*1) is calculated directly from the wavefunction; (*a*2), (*b*) and (*c*) are derived from the multipole-projected invariom database entries. (*a*1) and (*a*2) are (1); (*b*) is (2); (*c*) is (3).

molecules are compared can only be studied when an accurate structure together with the ESP of a receptor are available, in addition to the results presented here.

5. Conclusion

Aspherical scattering factors modelling the bonding electron density of organic compounds provide a powerful tool for the description of the electron density of larger molecules. Based on the invariom-model electron density, further properties can be derived. Here the ESPs derived for chemically related isoflavone molecules are compared in an attempt to provide information for understanding their bioactivity. The fit of the invariom structure factors to the observed low-temperature X-ray intensities measured for this study yields a molecular geometry of charge-density quality which is expected to agree better with theoretical and neutron results than with the IAM geometry.

A Japanese Society for the Promotion of Science Fellowship grant to one of us (RKA) to carry out research at Okayama University is gratefully acknowledged. We also thank Mr Shinetsu Igarashi and Dr Kenji Yoza of Bruker AXS KK for X-ray measurements and data reduction. This work was supported by the Australian Synchrotron Research Program (ASRP), which is funded by the Commonwealth of Australia under the Major National Research Facilities Program. BD thanks the ASRP for a postdoctoral fellowship and the Australian Partnership for Advanced Computing (APAC) for computing time.

References

Abbiw, D. (1990). *Useful Plants of Ghana*, London: Intermediate Technology Development Group and the Royal Botanical Gardens, Kew.
Abbott, W. S. (1925). *J. Econ. Entomol.* **18**, 265–267.
Brock, C. P. & Dunitz, J. D. (1982). *Acta Cryst.* B**38**, 2218–2228.
Bruker AXS Inc. (2002). *COSMO*. Bruker AXS Inc., Madison, Wisconsin, USA.
Burnett, M. N. & Johnson, C. K. (1996). *ORTEP*III. Report ORNL-6895. Oak Ridge National Laboratory, Tennessee, USA.
Chandler, G. S. & Spackman, M. A. (1978). *Acta Cryst.* A**34**, 341–343.
Coppens, P., Sabine, T. M., Delaplane, R. G. & Ibers, J. A. (1969). *Acta Cryst.* B**25**, 2451–2458.
Dittrich, B., Hübschle, C. B., Messerschmidt, M., Kalinowski, R., Girnt, D. & Luger, P. (2005). *Acta Cryst.* A**61**, 314–320.
Dittrich, B., Koritsánszky, T. & Luger, P. (2004). *Angew. Chem. Int. Ed.* **43**, 2718–2721.
Dittrich, B., Luger, P. & Spackman, M. A. (2006). To be published.
Frisch, M. J. *et al.* (1998). *GAUSSIAN*98, revision A.7. Gaussian, Pittsburgh, PA, USA.
Hansen, N. K. & Coppens, P. (1978). *Acta Cryst.* A**34**, 909–921.
Hirshfeld, F. L. (1976). *Acta Cryst.* A**32**, 239–244.
Hübschle, C. B. (2006). *MOLISO*. Freie Universität Berlin, Germany.
Hübschle, C. B. & Dittrich, B. (2004). *INVARIOMTOOL*. Freie Universität Berlin, Berlin, Germany.
Irvine, F. R. (1961). *Wood Plants of Ghana*, 1st ed. Oxford University Press.
Jayatilaka, D. & Grimwood, D. J. (2003). *Comput. Sci.* **2660**, 142–151.
Kingsford-Adaboh, R., Ahiano, E., Dittrich, B., Okamoto, H., Kimura, M. & Ishida, H. (2006). *Cryst. Res. Technol.* **42**, 728–733.
Kingsford-Adaboh, R., Osei-Fosu, P., Asomaning, W. A., Weber, M. & Luger, P. (2001). *Cryst. Res. Technol.* **36**, 107–115.
Koritsánszky, T., Richter, T., Macchi, P., Volkov, A., Gatti, C., Howard, S., Mallinson, P. R., Farrugia, L., Su, Z. W. & Hansen, N. K. (2003). *XD*. Freie Universität Berlin, Germany.
Koritsánszky, T., Volkov, A. & Coppens, P. (2002). *Acta Cryst.* A**58**, 464–472.
Kurki-Suonio, K. (1977). *Isr. J. Chem.* **16**, 115–123.
Lyddiard, J. R. A. & Whitfield, P. J. (2001). *J. Helminthol.* **75**, 1–7.
Lyddiard, J. R. A., Whitfield, P. J. & Bartlett, A. (2002). *J. Parasitol.* **88**, 163–170.
Maillard, M., Marston, A. & Hostettmann, K. (1993). *Human Medicinal Agents from Plants*, *American Chemical Society Symposium Series 534.* Washington: American Chemical Society.
Meyer, B. N., Ferrigni, N. R., Putnam, J. E., Jacobsen, L. B., Nichols, D. R. & McLaughlin, J. L. (1982). *Planta Med.* **45**, 31–34.
Sheldrick, G. M. (1990). *SHELXS*97. University of Göttingen, Germany.
Sheldrick, G. M. (1997). *SHELXL*97. University of Göttingen, Germany.
Su, Z. & Coppens, P. (1992). *Acta Cryst.* A**48**, 188–197.
Volkov, A., Li, X., Koritsánzky, T. & Coppens, P. (2004). *J. Phys. Chem. A*, **108**, 4283–4300.
Yenesew, A., Derese, S., Midiwo, J. O., Heydenreich, M. & Peter, M. G. (2003). *Pest Manage. Sci.* **59**, 1159–1163.